ResearchGate

See discussions, stats, and author profiles for this publication at:
https://www.researchgate.net/publication/256757608

# Effect of Al3+ and Ti4+ ions on the laser reduction of Sm3+ ion in glass

**ARTICLE** *in* JOURNAL OF LUMINESCENCE · SEPTEMBER 2005

Impact Factor: 2.72 · DOI: 10.1016/j.jlumin.2004.12.010

CITATIONS
12

READS
42

**5 AUTHORS**, INCLUDING:

M. Nogami
Toyota Physical and Chemical Researc…
**546** PUBLICATIONS **8,502** CITATIONS
SEE PROFILE

Go Kawamura
Toyohashi University of Technology
**79** PUBLICATIONS **595** CITATIONS
SEE PROFILE

Hongpeng You
Chinese Academy of Sciences
**178** PUBLICATIONS **3,403** CITATIONS
SEE PROFILE

Tomokatsu Hayakawa
Nagoya Institute of Technology
**152** PUBLICATIONS **2,187** CITATIONS
SEE PROFILE

Available from: Go Kawamura
Retrieved on: 24 January 2016

Available online at www.sciencedirect.com
SCIENCE DIRECT®
Journal of Luminescence 114 (2005) 178–186
JOURNAL OF LUMINESCENCE
www.elsevier.com/locate/jlumin

# Effect of $Al^{3+}$ and $Ti^{4+}$ ions on the laser reduction of $Sm^{3+}$ ion in glass

Masayuki Nogami*, Go Kawamura, Gil Jae Park, Hongpeng You, Tomokatsu Hayakawa

*Department of Material Science and Engineering, Nagoya Institute of Technology, Showa, Nagoya 466-8555, Japan*

Received 13 October 2004
Available online 1 June 2005

**Abstract**

Femtosecond laser pulses were used to change the valence of $Sm^{3+}$ ions doped in silicate glasses consisting of $Al_2O_3$ and $TiO_2$. When doped in $TiO_2$–$SiO_2$ glass, no change was observed in $Sm^{3+}$ ions by laser irradiation. On the other hand, $Sm^{3+}$ ions were reduced to $Sm^{2+}$ in $Al_2O_3$-containing glasses. Fluorescence line-narrowing spectra indicate that $Ti^{4+}$ ions are dissolved in silica network and occupy the tetrahedral site forming Si–O–Ti bonds, while $Al^{3+}$ ions occupy tetrahedral and octahedral sites. The laser irradiation carries to form the hole-defect centers in the oxygen ions in the Al–O octahedral. The released electrons from oxygen ions are captured in the nearest neighboring $Sm^{3+}$ ions, resulting in the formation of $Sm^{2+}$. On the other hand, in the $Ti^{4+}$-containing glasses, the electrons are trapped in $Ti^{4+}$ ions and no $Sm^{2+}$ ions are formed. The fluorescence properties of the $Sm^{2+}$ ions and defect centers were compared from the time-resolved fluorescence spectra.
© 2004 Elsevier B.V. All rights reserved.

*PACS:* 42.70.Ln; 71.20.Eh; 78.55.Qr

*Keywords:* Rare-earth; Laser; Valence change; Glass; Sol–gel

## 1. Introduction

Glasses doped with rare-earth ions have attracted significant attention because they can be used for the fabrication of photonic devices. In oxide glasses, the rare-earth elements usually take on the trivalent state and the 4f electrons are shielded by the 5s outer shells. According to these electron configurations, sharp absorption and emission lines are observed, which are appropriate for optical devices such as lasers and amplifiers. Some rare-earth ions can be presented as a valence other than the trivalent state, e.g., $Eu^{2+}$, $Sm^{2+}$, $Ce^{4+}$, and $Tb^{4+}$. Among them, the $Eu^{2+}$ and $Sm^{2+}$ ions are particularly interesting because they

*Corresponding author. Tel./fax: +81 527355285.
*E-mail address:* nogami@mse.nitech.ac.jp (M. Nogami).

0022-2313/$ - see front matter © 2004 Elsevier B.V. All rights reserved.
doi:10.1016/j.jlumin.2004.12.010

exhibit a large Faraday rotation effect [1], a long-lasting phosphorescence [2], and a photochemical persistent spectral hole burning [3,4]. One technique to reduce the rare-earth ions is the melting of glass at high temperature under a strong reducing atmosphere [3,5]. We used a sol–gel technique to prepare glasses doped with $Eu^{2+}$ and $Sm^{2+}$ ions [4]. The sol–gel process allows the rare-earth ions to be reduced at moderately low temperatures. The heating process is convenient for changing the valence of rare-earth ions throughout the sample, but is not appropriately used for the microscopic local modification of the glass. X-ray and laser beams have been used to change the properties of glasses at the focal points [6–13]. With respect to the microscopic modifications, X-ray and laser irradiations offer a greater advantage than the heating process.

Recently, Hirao's group successfully used near-IR femtosecond (fs) laser pulses to reduce the $Eu^{3+}$ and $Sm^{3+}$ ions in fluoride, silicate, and borate glasses, and reported the possibility of the three-dimensional site selective modification inside a transparent glass [7–10]. Of particular interest in this technique is the internal microstructuring of a glass without inducing a crack in the vicinity of the focal point of the laser beam. Thus, the fs-laser pulses have been recognized as an outstanding tool for the fabrication of three-dimensional integrated circuits. We also demonstrated the reduction of $Sm^{3+}$ ions into $Sm^{2+}$ doped in the sol–gel $Al_2O_3$–$SiO_2$ glasses by irradiation with fs-laser beams and X-rays, and found that the hole-burning efficiency of $Sm^{2+}$ ions is superior to that in hydrogen-treated glasses [14,15]. Through our experimental experience, we noticed that the nature of the host glass composition plays an important role in reducing $Sm^{3+}$ ions [16]. When doped in $SiO_2$ glass, the $Sm^{3+}$ ions cluster and are hardly reduced to $Sm^{2+}$, even when irradiating with a high power of laser. The $Ti^{4+}$ ion has the same effect of not reducing the rare-earth ions. The $Al^{3+}$ ion is the only promising one for the reduction of $Sm^{3+}$ ions. However, it is not very clear how these co-doped cations contribute to the reduction of the rare-earth ions in host glasses.

In this paper, we discuss the effect of $Al^{3+}$ and $Ti^{4+}$ ions on the reduction of $Sm^{3+}$ ions during the fs-laser irradiation. The $Sm^{3+}$ ions were doped in $Al_2O_3$–$TiO_2$–$SiO_2$ glasses using the sol–gel method and the laser reduction of $Sm^{3+}$ was measured as a function of the $Al_2O_3$ content in the glasses. The reduction of $Sm^{3+}$ to $Sm^{2+}$ was related to the chemical bonding of the oxygen–polyhedra surrounding the $Sm^{3+}$ ions.

## 2. Experimental

$Al_2O_3$–$TiO_2$–$SiO_2$ glasses doped with 10 wt% $Sm_2O_3$ were prepared by the sol–gel method using $Si(OC_2H_5)_4$, $Al(OC_4H_9^{sec})_3$, $Ti(OC_4H_9)_4$, $SmCl_36H_2O$, deionized water, and ethanol as the starting materials. $Si(OC_2H_5)_4$ was first hydrolyzed with a mixed solution of ethanol and deionized water. A small amount of HCl solution was added as a catalyst. $Al(OC_4H_9^{sec})_3$ was then added to the partially hydrolyzed $Si(OC_2H_5)_4$, followed by stirring for 1 h at about 70 °C. After cooling to room temperature, $Ti(OC_4H_9)_4$ was added and stirred for 1 h, and then $SmCl_36H_2O$ dissolved in ethanol was added to this solution and stirred for another 30 min. The mixed solution of $H_2O$ and $C_2H_5OH$ was added for the final hydrolysis of the alkoxides, followed by stirring for 1 h. The obtained homogeneous solutions were cast into plastic containers, where they were allowed to gel at room temperature. The obtained gels were heated at 500 °C in air for 2 h, polished and further heated at 800 and 1000 °C in air for 2 h. The $10Al_2O_3$–$90SiO_2$ and $10TiO_2$–$90SiO_2$ glasses doped with $Eu_2O_3$ were also prepared using $EuCl_36H_2O$ to measure the fluorescence properties.

The fs pulse laser irradiation of the glasses was performed by a Ti:sapphire regenerative amplifier laser system (Spectra Physics, Hurricane) operating at a wavelength of 800 nm with a 1 kHz repetition rate and 130 fs pulse duration. A laser beam with an average power of 780 mW irradiated the sample for 3 min through an objective lens with a 30 cm focusing length. Optical focusing was moved 3–5 mm from the sample in order not to damage the sample.

The optical absorption spectra were measured using a spectrometer (Jasco, V-570) in the wave-

length range from 200 to 900 nm. The fluorescence (FL) spectra were recorded using a $N_2$ laser (Laser Photonics, Inc., LN203C: pulse width ~1 ns) with a 337 nm wavelength for excitation. The $N_2$ laser was overlapped with the fs laser-irradiated area using the objective lens. The fluorescence was led to a monochromator (Jobin Yvon, HR 320) through an optical fiber and detected by the ICCD camera (Oriel Instruments, InstaSpec V System). The delay time for the ICCD gate pulse was changed depending on the fluorescence lifetime. The fluorescence line narrowing (FLN) spectra were obtained by exciting the $^7F_0 \rightarrow {}^5D_0$ transition of both the $Sm^{2+}$ and $Eu^{3+}$ ions.

The electron spin resonance (ESR) spectra were obtained at 123 K by applying an X-band microwave frequency (Jasco, JES-RE1X). The quoted $g$-values were referenced to the value for diphenylpicrylhydrazal (DPPH).

## 3. Results and discussion

### 3.1. Formation of $Sm^{2+}$ ions in $TiO_2$–$Al_2O_3$–$SiO_2$ glasses

The glasses obtained by heating gels in air were transparent and showed optical absorption spectra characteristic of the f–f transition of $Sm^{3+}$ ions. The $Sm_2O_3$ content remained constant at 10 wt% and the observed optical absorption intensities of the $Sm^{3+}$ ions were almost the same and independent of the composition of the host glass. On the other hand, the fluorescence properties are strongly affected by the local structure surrounding the $Sm^{3+}$ ions. The emission bands due to the f–f transitions within $Sm^{3+}$ $4f^5$ configuration appear at about 550, 600, and 650 nm, the intensities of which were significantly dependent on the $TiO_2$ and $Al_2O_3$ contents. The emission intensity increased with the increasing $Al_2O_3$ content and the intensity in the $10Al_2O_3$–$90SiO_2$ glass was ten times higher than that in the $10TiO_2$–$90SiO_2$ glass.

Previously, we studied the fluorescence properties of $Eu^{3+}$ ions in $SiO_2$, $TiO_2$–$SiO_2$ and $Al_2O_3$–$SiO_2$ glasses [17,18]. In $SiO_2$ glass, $Eu^{3+}$ ions have a tendency to cluster, resulting in an emission quenching. When $TiO_2$ is introduced into the silica glass, the emission intensity of $Eu^{3+}$ ions was found to increase. The $Ti^{4+}$ ions are dissolved in the silica network and occupy tetrahedral sites forming Si–O–Ti bonds. Considering the fact that the $Ti^{4+}$ ion has a larger size and a smaller electronegativity compared with the $Si^{4+}$ ion, the $Eu^{3+}$ ions are preferentially bonded with the $Ti^{4+}$ ions to form $Eu^{3+}$–O–$Ti^{4+}$ bonds, which leads to reducing the extent of $Eu^{3+}$ clusters and enhancing the emission intensity. However, we found that the network structure consisting of $TiO_2$ is very similar to that of silica glass within a $TiO_2$ content of 15% [18]. Therefore, it is suggested that $Eu^{3+}$ ions still have a tendency to form clusters, although $Ti^{4+}$ ions can reduce the extent of $Eu^{3+}$ clusters. On the other hand, we found that the emission intensity of $Eu^{3+}$ ions is significantly enhanced by the incorporation of $Al_2O_3$ in silica glass [17]. The $Al^{3+}$ ions can occupy tetrahedral and octahedral sites in the glass structure, where $Al^{3+}$ ions in the octahedral site effectively act to reduce $Eu^{3+}$ clusters, resulting in enhanced emission intensity.

Fig. 1 shows the FL spectra of $10Al_2O_3$–$90SiO_2$ and $5Al_2O_3$–$5TiO_2$–$90SiO_2$ glasses before and after fs-laser irradiation. The FL spectra were taken in the visible wavelength region using a 337 nm excitation wavelength of a $N_2$ laser at room temperature. Before the laser irradiation, both glasses exhibit sharp FL bands at 567, 604 and 654 nm, which are all assigned to the $^4G_{5/2} \rightarrow {}^6H_{5/2,7/2,9/2}$ transitions, respectively, of $Sm^{3+}$ ions, while their intensities are weaker for $5Al_2O_3$–$5TiO_2$–$90SiO_2$ glass. When irradiated with the fs-laser in $5Al_2O_3$–$5TiO_2$–$90SiO_2$ glass, no change was observed, even with a slight increase in the wavelength below about 550 nm. The origin of this 550 nm fluorescence will be discussed in Section 3.4. The same spectral features were observed for glasses containing less than 5% $Al_2O_3$ in the system $xAl_2O_3$–$(10-x)TiO_2$–$90SiO_2$.

On the other hand, in glasses containing $Al_2O_3$ $>5\%$, new FL lines appeared for the long wavelengths at 680–730 nm, and their intensities increased as the $Al_2O_3$ content increased. These new bands at 680, 710, and 730 nm are assigned to the $^5D_0 \rightarrow {}^7F_{0,1,2}$ transitions of $Sm^{2+}$

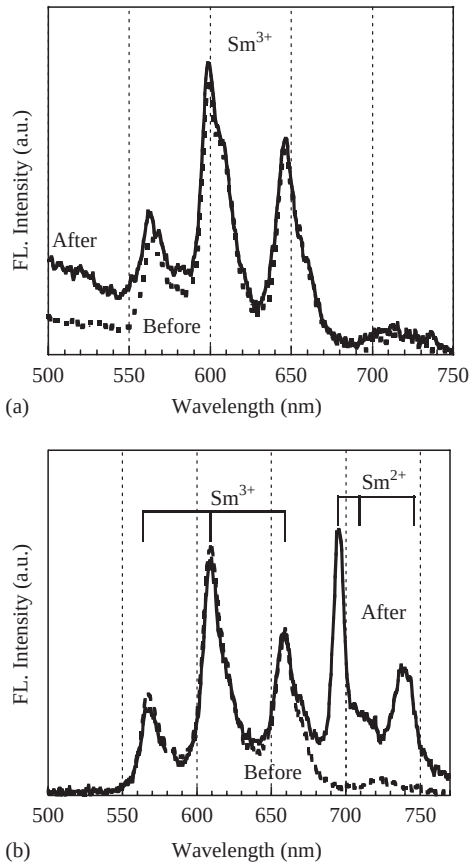


Fig. 1. Fluorescence spectra of $Sm^{3+}$-doped $5Al_2O_3$–$5TiO_2$–$90SiO_2$ (a) and $10Al_2O_3$–$90SiO_2$ (b) glasses before (dotted line) and after (solid line) fs laser irradiation.

ions, respectively. Thus, it is concluded that $Sm^{3+}$ ions are reduced by fs-laser irradiation and their reduction is strongly affected by the host glass. The FL intensities of $Sm^{2+}$ and $Sm^{3+}$ ions, denoted as $I_2$ and $I_3$, respectively, are determined as the area of FL-bands of the $^5D_0 \rightarrow {}^7F_{0,1,2}$ ($Sm^{2+}$) and $^4G_{5/2} \rightarrow {}^6H_{5/2,7/2,9/2}$ ($Sm^{2+}$) transitions, which are plotted as a function of the $Al_2O_3$ content in Fig. 2. It is apparent that the reduction of $Sm^{3+}$ ions is increased by the addition of $Al^{3+}$ ions.

### 3.2. Formation process of $Sm^{2+}$ ions by laser irradiation

We have studied the reduction of $Sm^{3+}$ ions in the glasses prepared by heating under a hydrogen

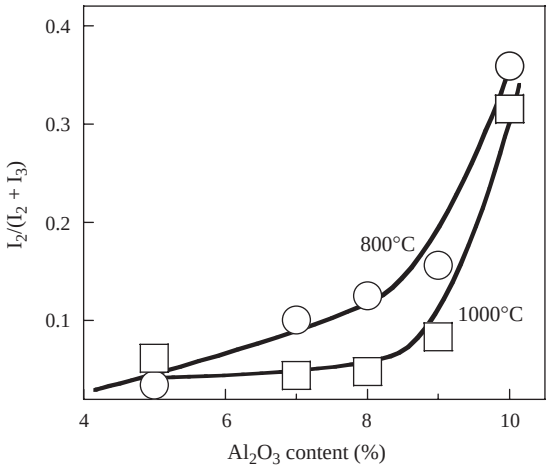


Fig. 2. Fluorescence intensity ratio of $Sm^{2+}$ and $Sm^{3+}$ ions in $xAl_2O_3$–$(10-x)TiO_2$–$90SiO_2$ glasses irradiated with laser.

atmosphere [4] or irradiating with X-ray [6] and laser pulses [14]. In the glass heated in $H_2$ gas, $H_2$ molecules deplete the oxygen ions surrounding $Sm^{3+}$ ions, resulting in the formation of $Sm^{2+}$ ions. In contrast, in the X-ray-irradiated glass, $Sm^{3+}$ ions are not reduced by the removal of coordinated-oxygen ions, but by the electron transfer between oxygen and $Sm^{3+}$ ions. Compared with these reduction processes, the fs-laser process seems to resemble that of the X-rays. In Fig. 3, the ESR spectra of the laser-irradiated glasses are shown. The laser-irradiated $10Al_2O_3$–$90SiO_2$ glass shows ESR signals at around 3200–3300 G with $g = 2.009$ and fine hyperfine structures. We assigned these ESR signals to the hole centers trapped in oxygen ions bound with Al ions (so-called Al–OHC) [19]. On the other hand, the $Al_2O_3$ and $TiO_2$-codoped glasses exhibit a very broad signal at around 3400 G in addition to the Al–OHC signal. We found that the intensity of the 3400 G signal increases as does the $TiO_2$ content, reaching the maximum at a composition of $5Al_2O_3$–$5TiO_2$–$90SiO_2$. No signal was observed in the $10TiO_2$–$90SiO_2$ glass. Compared with that of the free electron ($g = 2.00232$), the 3400 G signal ($g = 1.9483$) can be assigned to the electron-trap centers. Based on these experimental results and analogy to that of the X-ray irradiated glass, we can consider the effect of $Ti^{4+}$ and $Al^{3+}$ ions on the reduction of $Sm^{3+}$ ions.

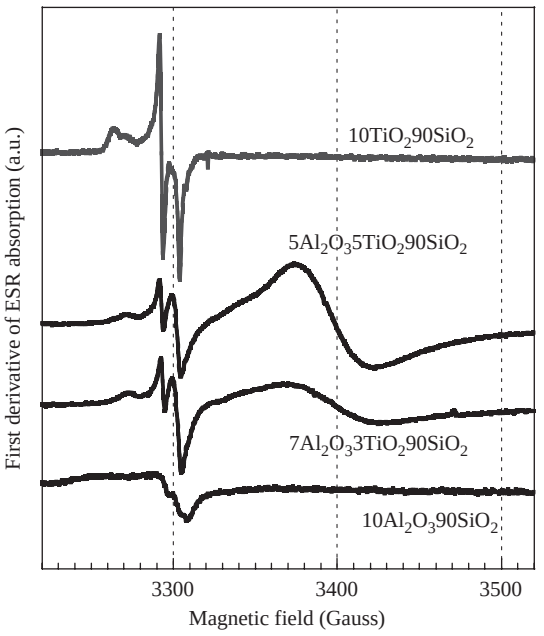


Fig. 3. ESR spectra of laser-irradiated $x Al_2O_3$–$(10-x)TiO_2$–$90SiO_2$ glasses.

$Sm^{3+}$ ions are preferentially bound with Al–O polyhedra, in which $Al^{3+}$ ions occupy tetrahedral and octahedral sites in the glass structure, bonding with the 4 and 6 oxygens, respectively. Therefore, it is reasonable to conclude that $Sm^{3+}$ ions are reduced to $Sm^{2+}$ by the electron transfer between oxygen and samarium ions. The octahedrally bonded Al–O polyhedra are damaged during the laser irradiation, resulting in the formation of hole-defect centers in the oxygen ions bound to $Al^{3+}$ ions(Al–OHC). The released electrons from the oxygen ions are captured by the nearest neighboring $Sm^{3+}$ ions to reduce them to $Sm^{2+}$. The $Sm^{3+}$ ions act as an electron acceptor. However, when co-existing with $Ti^{4+}$ ions, the electrons are preferably captured by $Ti^{4+}$ ions. Thus, it is concluded that $Al^{3+}$ ions are appropriate for the reduction of $Sm^{3+}$ ions in the glass matrix.

### 3.3. Effect of $Al^{3+}$ and $Ti^{4+}$ ions on local structure surrounding the rare-earth ions

It is evident that $Al^{3+}$ and $Ti^{4+}$ ions have different effects on the reduction of $Sm^{3+}$ ions. In this section, we discuss the local structure of $Sm^{3+}$ ions using the fluorescence line-narrowing technique. The technique of laser-induced fluorescence narrowing provides a microscopic probe of the local environment around the rare-earth ions. The $Sm^{3+}$ ion has a ground state of the $^6H_{5/2}$ level, in which the crystal field is splitting. On the other hand, the $Sm^{2+}$ and $Eu^{3+}$ ions have the same $4f^6$ electron configuration and can be considered to have a similar effect on the glass structure, although there is a slight difference in their sizes. The ground and lowest excited levels of these ions are $^7F_0$ and $^5D_0$, respectively, and the $^5D_0 \rightarrow {}^7F_0$ transition exhibits no crystal field splitting, thus making the assignment of the fluorescence spectra much simpler. Therefore, the crystal-field analysis of the FLN spectra as a function of the excitation wavelength within the $^5D_0 \rightarrow {}^7F_0$ transition can provide an insight into the local structure. To study the effect of $Al^{3+}$ and $Ti^{4+}$ ions on the chemical features of the trivalent rare-earth ions, the FLN spectra were measured using the $Eu^{3+}$ ion as the prove ion, which are shown in Fig. 4 in the range from 570 to 620 nm wavelength. In $TiO_2$–$SiO_2$ glass (see Fig. 4(a)), three groups of lines, observed at ~17,250, 17,000–16,600, and 16,500–15,900 $cm^{-1}$, are assigned to the $^5D_0 \rightarrow {}^7F_0$, $^5D_0 \rightarrow {}^7F_1$, and $^5D_0 \rightarrow {}^7F_2$ transitions, respectively. Among these lines, three distinct peaks in the $^5D_0 \rightarrow {}^7F_1$ transition are due to the Stark splitting of the $^7F_1$ level, indicating that $Eu^{3+}$ ions are located at one site with the symmetry of $C_{2v}$, or lower. It is apparent that no change is observed in the spectral shape and peak positions of the $Eu^{3+}$-doped $TiO_2$–$SiO_2$ glass. This behavior is similar to that observed in the silica glass doped with $Eu^{3+}$ ions. The absence of the line-narrowing effect indicates the clustering of $Eu^{3+}$ ions, where an efficient energy transfer has taken place within $Eu^{3+}$ ions. This strongly suggests that although $Ti^{4+}$ ions replace $Si^{4+}$ to form Si–O–Ti bonds, the network structure is very similar to that of silica glass, which does not contribute to decreasing the clustering of $Eu^{3+}$ ions.

In contrast to $Eu^{3+}$-doped $TiO_2$–$SiO_2$ glass, $Eu^{3+}$-doped $Al_2O_3$–$SiO_2$ glass shows a quite different behavior in the FLN spectra as shown in Fig. 4(b). In the FLN spectrum for the 17,250 $cm^{-1}$ excitation, the $^5D_0 \rightarrow {}^7F_1$ band is

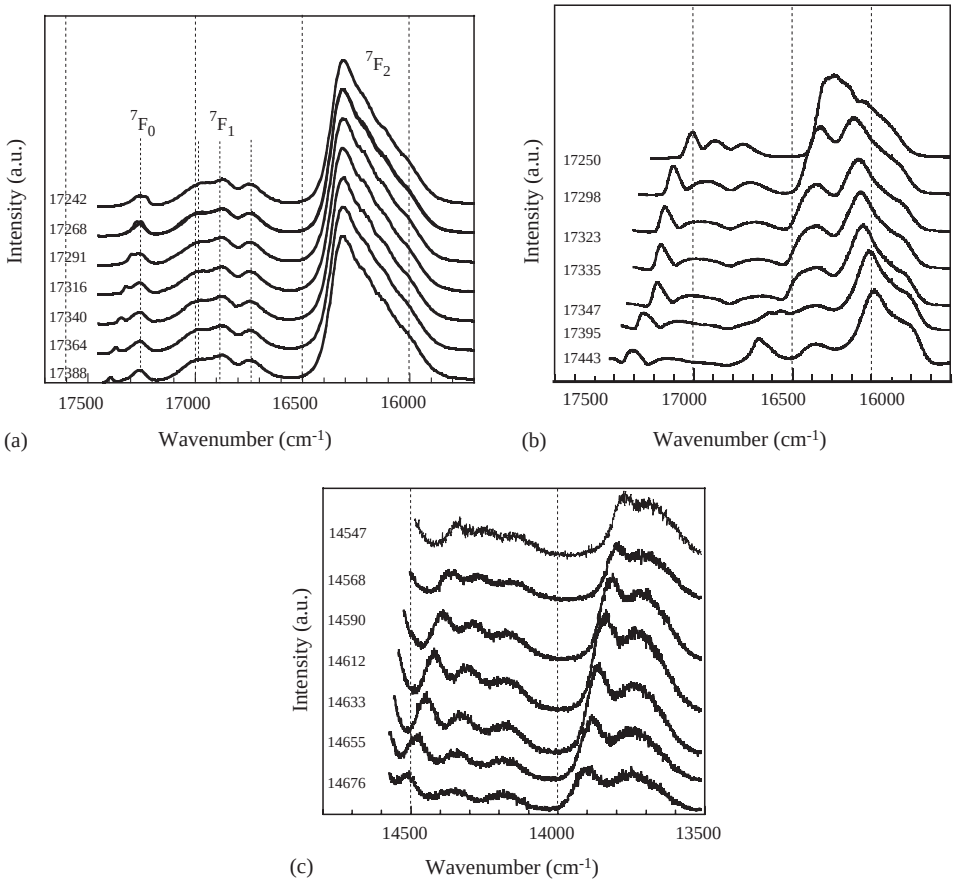


Fig. 4. FLN spectra of $Eu^{3+}$ and $Sm^{2+}$ ions doped in glasses. The $10TiO_2$–$90SiO_2$ (a) and $10Al_2O_3$–$90SiO_2$ (b) glasses doped with $Eu^{3+}$ ions are heated in air atmosphere. The $Sm^{2+}$-doped $10Al_2O_3$–$90SiO_2$ glass was obtained by irradiating with fs laser (c). The numbers are the excitation wavenumber in $cm^{-1}$.

clearly split into three lines. The position of the three splitting lines separately shifts to the opposite side with increasing excitation energy and other new components begin to be observed at around 16,900 and 16,600 $cm^{-1}$ during the 17,335 $cm^{-1}$ excitation. Concomitantly, it is noticed that in the $^5D_0 \rightarrow {}^7F_2$ transition region, a new broad band appears at around 16,200 $cm^{-1}$ and the intensity of this line increases with increasing excitation energy. These phenomena suggest the existence of two chemical components surrounding the $Eu^{3+}$ ions. On the basis of this consideration, the broad $^5D_0 \rightarrow {}^7F_1$ transition bands were deconvoluted using a Gaussian distribution function and the peak positions of each band were determined, which are plotted in Fig. 5(a) as a function of the excitation energy. Note that the $^7F_1$ components can be classified into two groups (open and closed marks in Fig. 5(a)), indicating that the $Eu^{3+}$ ions are surrounded by two different Al–O polyhedra in the $Al_2O_3$–$SiO_2$ glass structure. It is known that the $Al^{3+}$ ion is 4- and/or 6-coordinated with oxygen ions in the alkali–aluminosilicate glasses [20]. The 4-coordinated $Al^{3+}$ ion forms the Si–O–Al network structure, where the negative charge of the $AlO_4$ tetrahedra is compensated by the accompanying alkali ion. In contrast, our glasses contain no alkali oxides, and the $Eu^{3+}$ ion is too large to enter the $AlO_4$ network structure. Consequently, the $Eu^{3+}$ ion acts as a

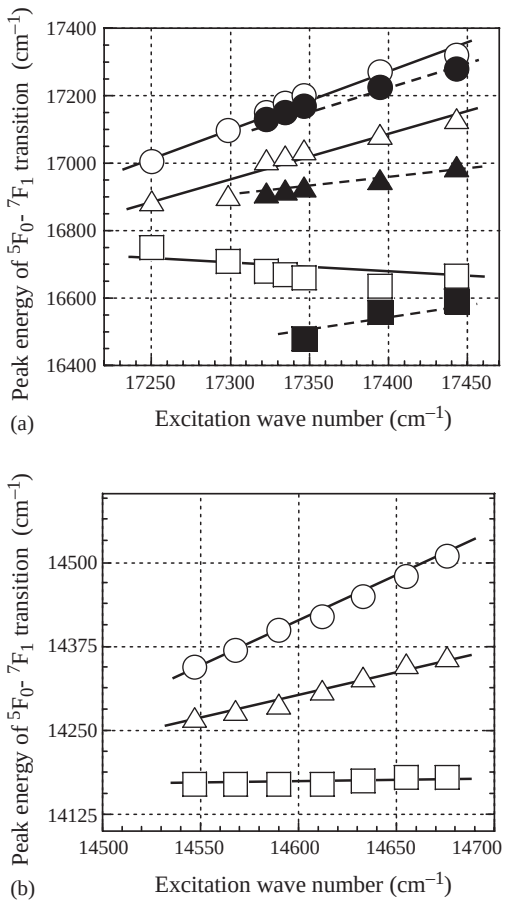


Fig. 5. Peak energies of three $^5D_0 \rightarrow {}^7F_1$ fluorescence lines of $Eu^{3+}$ ions (a) and $Sm^{2+}$ ions (b) doped in $10Al_2O_3$–$90SiO_2$ glasses as a function of $^7F_0 \rightarrow {}^5D_0$ excitation energy.

network modifier ion in the glass and its positive charge is compensated by the non-bridging oxygens bonded to the $AlO_6$ octahedra. A similar chemical bonding can take place in the $Sm^{3+}$ ion-doped glasses.

Fig. 4(c) shows the FLN spectra of $Sm^{2+}$ ions in $Al_2O_3$–$SiO_2$ glass, in which $Sm^{3+}$ ions are changed into $Sm^{2+}$ by fs-laser irradiation. Note that only three lines are observed in the $^5D_0 \rightarrow {}^7F_1$ transition region. This result indicates that $Sm^{3+}$ ions located in two different sites are not similarly reduced to $Sm^{2+}$. The peak shift of the three lines with increasing excitation energy resembles that for the second site observed in the $Eu^{3+}$-doped $Al_2O_3$–$SiO_2$ glass, as shown in Fig. 5(b), suggesting that the $Sm^{3+}$ ions bound with the octahedral $AlO_6$ groups are selectively reduced to $Sm^{2+}$.

### 3.4. Fluorescence properties of $Sm^{2+}$ ions in $Al_2O_3$–$SiO_2$ glass

The fs-laser pulses with a high intensity are known to produce free electrons in a glass via multiphoton absorption and the avalanche ionization leads to plasma generation, resulting into the formation of defect centers in a glass [14]. Therefore, it is necessary to consider the optical absorption and fluorescence from the defect centers in addition to the rare-earth ions. Laser irradiation induces a broad optical absorption between 300 and 600 nm, which is ascribed to the $4f^6 \rightarrow 4f^5 5d$ transition of $Sm^{2+}$ ions. The $4f^5 5d$ configuration has a wide distribution in energy and exhibits an absorption band overlapped with the $4f^6$ levels and the defect centers in the host structure. The $Al_2O_3$–$SiO_2$ host glass also has a strong absorption below ~270 nm due to the fundamental absorption of the glass structure. Therefore, the $N_2$ laser at 337-nm wavelength, used for the measurement of the emission spectra, excites electrons in the different components and produces complex fluorescence properties.

The fluorescence spectra were measured in detail by changing the gate time of the opening ICCD camera. Shown in Fig. 6 are the typical FL spectra in the visible wavelength region. A broad FL band peaking at ~460 nm exhibits the very short lifetime of 20 ns (see the decay curve shown in the inset of Fig. 6(a)). Some possible origins for this FL band can be considered: the radiative relaxation from the $4f^5 5d$ to $4f^6(^7F_0)$ level of $Sm^{2+}$ ions, and the existence of defect centers. Generally it is known that the divalent rare-earth ions exhibit lifetimes on the ns order. Compared with this lifetime, the FL band at 460 nm might be assigned to the $4f^5 5d \rightarrow 4f^6$ transition of $Sm^{2+}$. However, the emission from the defect centers is not rejected at present; therefore further study is needed.

Fig. 6(b) shows the FL spectrum measured with a 70 μs gate width. It is noticed that the sharp FL lines due to the $^5D_0 \rightarrow {}^7F_{0,1,2}$ transitions of the $Sm^{2+}$ ions are superpositioned on a broad band

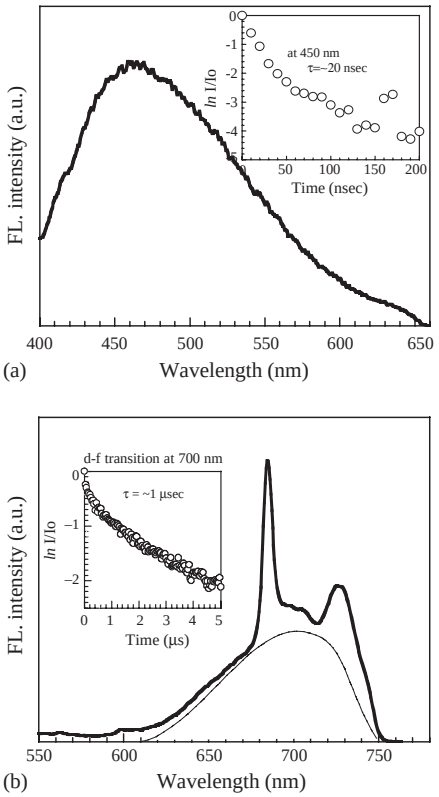


Fig. 6. Fluorescence spectra of $Sm^{2+}$ ion-doped $10Al_2O_3$–$90SiO_2$ glasses, measured with 10 ns (a) and 70 μs (b) gate width.

peaking at ~700 nm. Since the lifetime of the f–f transition is usually of the order of milliseconds, a short gate width time was used to detect the broad fluorescence. In the inset of Fig. 6(b) is shown the decay curve of the FL intensity at 700 nm, the lifetime of which is estimated to be 1 μs. He et al. observed a similar broad fluorescence in the $BaCl_2$ crystal doped with $Sm^{2+}$ ions and assigned to the two-step quenching model via the 5d level [21]. Based on these experimental results, the energy-level diagram of the $Sm^{2+}$ ions and a possible pathway for the excited energy is schematically drawn in Fig. 7. The excited electrons in the level of the 4f5d configuration non-radiatively relax into the lowest energy $^5D_0$ level and radiatively transfer into the ground $^7F_j$ level. A part of the excited electrons are relaxed within the 5d orbital, followed by the radiative 5d–4f transition.

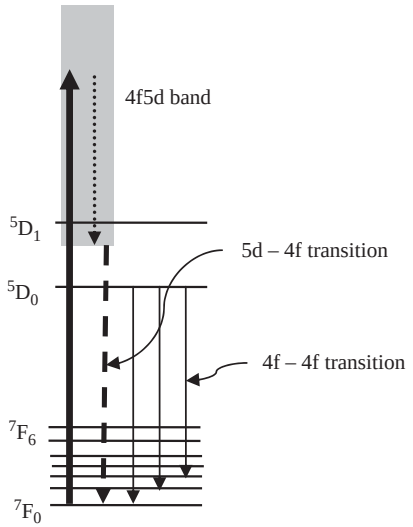


Fig. 7. Schematical energy diagram for $Sm^{2+}$ ions doped in glass.

## 4. Conclusion

In this study, the laser reduction of $Sm^{3+}$ ions in sol–gel glasses was investigated. We found that $Sm^{3+}$ ions are reduced to $Sm^{2+}$ in glasses containing $Al_2O_3$, whereas no $Sm^{2+}$ is formed in $TiO_2$-containing glasses. The chemical structure of the glass surrounding rare-earth ions was studied using the FLN spectra of $Eu^{3+}$ ions. The variation in the FLN spectra with the excitation energy reveals that $Ti^{4+}$ ions occupy tetrahedral sites within the silica network and act to capture the electron released by the laser irradiation, indicating no capability to reduce $Sm^{3+}$ ions. On the other hand, the FLN spectra of the $Al^{3+}$ ion-containing glasses show that $Eu^{3+}$ ions have two sites, one of which exhibits a large line-narrowing effect, and acts to form non-bridging oxygen ions in the Al–O polyhedra. Hole centers are formed in these oxygens by laser irradiation, and the released electrons are captured by $Sm^{3+}$ ions, thus resulting in the formation of $Sm^{2+}$.

## Acknowledgments

We thank the 21st century COE program of Nagoya Institute of Technology.

## References

[1] T. Hayakawa, M. Nogami, Solid State Commun. 116 (2000) 77.
[2] T. Matsuzawa, Y. Aoki, N. Takeuchi, Y. Murayama, J. Electrochem. Soc. 143 (1996) 2670.
[3] K. Hirao, S. Todoroki, D.H. Cho, N. Soga, N. Opt. Lett. 18 (1993) 1586.
[4] M. Nogami, Y. Abe, K. Hirao, D.H. Cho, Appl. Phys. Lett. 66 (1995) 2952.
[5] T. Izumitani, S.A. Payne, J. Lumin. 54 (1993) 337.
[6] M. Nogami, K. Suzuki, Adv. Mater. 14 (2002) 923.
[7] K.M. Davis, K. Miura, N. Sugimoto, K. Hirao, Opt. Lett. 21 (1996) 1729.
[8] J. Qiu, K. Miura, T. Suzuki, T. Mitsuyu, K. Hirao, Appl. Phys. Lett. 74 (1999) 10.
[9] J. Qiu, K. Miura, K. Nouchi, T. Suzuki, K. Kondo, T. Mitsuyu, K. Hirao, Solid State Commun. 113 (2000) 341.
[10] J. Qiu, K. Kojima, A. Kubo, M. Yamashita, K. Hirao, Phys. Chem. Glasses 41 (2000) 150.
[11] M. Watanabe, S. Juodkazis, H.-B. Sun, S. Matsuo, H. Misawa, Appl. Phys. Lett. 74 (1999) 3957.
[12] E.N. Glezer, M. Milosavlijevic, L. Huang, R.J. Finley, T.-H. Her, J.P. Callan, E. Mauzer, Opt. Lett. 21 (1996) 2023.
[13] C.B. Schaffer, A. Brodeur, J.F. Garcia, E. Mazur, Opt. Lett. 26 (2001) 93.
[14] G.J. Park, T. Hayakawa, M. Nogami, J. Phys. Condens. Matter. 15 (2003) 1259.
[15] G.J. Park, T. Hayakawa, M. Nogami, J. Lumin. 106 (2004) 103.
[16] M. Nogami, N. Hayakawa, N. Sugioka, Y. Abe, J. Am. Ceram. Soc. 79 (1996) 1257.
[17] M. Nogami, T. Nagakura, T. Hayakawa, T. Sakai, Chem. Mater. 10 (1998) 3991.
[18] H. You, M. Nogami, J. Phys. Chem. B 108 (2004) 12003.
[19] E.J. Friebele, D.L. Grisco, in: M. Tomozawa, R.H. Doremus (Eds.), Treatise on Materilas Science and Technology, vol. 17, Academic Press, New York, 1979, p. 257.
[20] W.D. Kingery, H.K. Bowen, D.R. Uhlmann, Introduction to Ceramics, second ed., Wiley, New York, 1976, p. 91.
[21] Zy. He, Ys. Wang, S. Li, Xr. Xu, J. Lumin. 97 (2002) 102.